A New Neural Network-Based Adaptive Time-Delay Control for Nonlinear Car Active Suspension System

Ghazally I. Y. MUSTAFA[1]*, Xinian LI[1], Haoping WANG[2]

[1] School of Information and Electronic Engineering, Shandong Technology and Business University, 191 Binhai Middle Road, Yantai, 264005, China
ghazally120@gmail.com (**Corresponding author*), xnli@sdtbu.edu.cn

[2] School of Automation, Nanjing University of Science and Technology Nanjing, 210094, China
hp.wang@njust.edu.cn

Abstract: This paper presents a new controller for a nonlinear active vehicle suspension system, based on a combination between a time-delay control and adaptive neural network control (TDANNC). The main objective is to deal with a classical conflict between enhancing the comfort of the car, and at the same time, keeping the ride safety within acceptable safety limits. Based on time-delay control, the nonlinearity of the model and the external disturbances are replaced. Besides, a radial basis function neural network is added to time-delay control in order to obtain a compelling tracking trajectory. Moreover, an adaptive law mechanism is used to achieve excellent overall performance across various road profiles, which can quickly and precisely adjust the neural network control gain online based on the control error. The advantage of TDANNC is that it is quite a simple structure and can easily be regulated due to a smaller model. Using the Lyapunov theory, the theoretical study demonstrates the stability and finite-time convergence of the system. Finally, to demonstrate the performance of the proposed TDANNC, it is compared to the performances of the conventional passive system, of TDC, of PID, and of NNC controllers under three distinct road disturbances. The simulation results are carried out to show the success and efficiency of the suggested strategy.

Keywords: Active suspension system, Time-Delay Control (TDC), Adaptive Neural Network (ANN), Time-Delay Estimation (TDE).

1. Introduction

The suspension system is an essential component of the car since it determines how comfortable the passengers ride and how well the car holds the road, which is essential for the ride's safety. The spring and damper are installed parallel to each other between the wheel and the body of the vehicle, to form the vehicle suspension system, which supports the connection between the body of the car and its wheels. It is necessary to separate the body from road disturbances to increase ride quality, which is the primary challenge of suspension system regulation. Moreover, to improve ride stability, it is essential to maintain tire contact with the road. With soft damping and larger suspension deflection, the optimal isolation of the sprung mass from road disturbances can be achieved for a given suspension spring. However, the best road contact can be attained by eliminating unwanted suspension deflections with stiff damping. Consequently, the quality of the ride and the stability of the vehicle are separate considerations (Mustafa, Wang & Tian, 2020).

Based on the simplified vehicle model, commercial vehicles use the passive suspension system to control their vertical motion dynamics. The passive suspension system limits the relative velocities of the body and of the wheels of the car, in order to provide the required ride characteristics. The disadvantage of passive suspension systems is that they cannot change their dynamics in real-time in response to the forces created by the irregular terrain. In contrast, semi-active and active suspension models have been developed to restrict these undesirable movements through masses with changeable dynamics (He et al., 2021). Semi-active suspensions are those in which the stiffness coefficient of the elastic element and the damping coefficient of the damper element can be adjusted to meet the needs of control and regulation. Active suspension systems use a moving part called an actuator to put the right amount of force between the body of the car and the wheel axle. Furthermore, despite the fact that an active suspension system consumes a significant amount of power (Long et al., 2020), it is widely acknowledged that it is an effective method for controlling the trade-off between competing performances and improving suspension performance. Also, automakers face a problem when they try to make driving safer and more comfortable: high-performance suspension systems can be made only with expensive and complicated energy-efficient systems. Nevertheless, suspension systems have a major impact on the subjective feeling of the car (Sun et al., 2014). Even though active suspensions can considerably improve ride comfort and safety

https://doi.org/10.24846/v31i4y202202

during travel, designing control algorithms for the active suspension system of a vehicle remains a challenge (Cao, Li & Liu, 2010).

In recent years, many diverse control techniques have been developed, such as H∞ optimum control (Wang et al., 2015), linear parameter varying feed-forward control (Fleps-Dezasse et al., 2018), backstepping control (Hu & Lin, 2008), and the LQR control (Gokul Prassad & Malar Mohan, 2019). The above methods suffer from several drawbacks since they rely on model-based control, which requires the creation of a mathematical model describing the dynamics of the model and applying analytical techniques to this model to generate suitable control laws. Nonlinear partial differential equations constitute the bulk of such mathematical models and are often used to describe physical phenomena. Moreover, most of the control strategies mentioned before are based on accurate known models. Nevertheless, these controllers may be sufficient for the suspension system and may give decent trajectory tracking. However, the fundamental concern with these control systems is that the inescapable presence of parametric errors, the truncation of high-order vibration modes, and the unknown road disturbances may worsen the vibration attenuation (Mustafa, Wang & Tian, 2019b).

Numerous advanced active suspension control approaches, such as sliding mode control (Mustafa, Wang & Tian, 2020), adaptive control techniques (Pan et al., 2017), intelligent control techniques (Shehata, Metered & Oraby, 2015), and hybrid-based advanced control (Zhao et al., 2016), have been presented to meet the performance criteria. The control strategy may be reliable and stable enough to counteract the nonlinearities of the model like parameter changes and/or outside disturbances. However, the control algorithms used in these systems have become increasingly complex, necessitating massive calculations to be performed in real-time.

In this paper, a simple and effective control design is proposed to improve performance tracking and overcome the uncertainties of the nonlinear mathematical model. First, time delay control (TDC) is utilized, which has two parts: the time-delay estimation (TDE) component meant to cancel nonlinearities and uncertainties of the active suspension system and the dynamic target component meant to insert desired error dynamics into the plant (Jin et al., 2017). Due to the TDE technique, a little knowledge regarding the suspension model of the car is required based on the presumption that the unknown nonlinear function does not change considerably over a short enough time. Unfortunately, the estimated error in TDE appears because of measurement noise and discontinuous nonlinearities (Xia et al., 2016). Second, to overcome the TDE shortcoming, an auxiliary radial basis function neural network (RBFNN) control is added as a powerful tool to reduce the TDE estimation error and improve the robustness and accuracy of the model output. Also, RBFNN has been widely used because it has a simple structure, good approximations, and can learn faster. Finally, the adjustability of the actuator components is the most important advantage of active suspension systems. If this flexibility is not used, i.e., if the control gain is selected as a constant, this will cause active suspension performance degradation under time-varying disturbances or tasks. To avoid this, an adaptive control law is combined with the RBFNN to adjust gains during operation. The essential advantage of the proposed controller is that it is easy to implement and design because it has a simple control structure. Besides, it has superior tracking accuracy and is insensitive to unforeseen disturbances. The entire control approach suggested in this paper will be referred to as Neural Network-Based Adaptive Time-Delay Control (TDANNC).

The rest of this work is organized as shown below. Section 2 outlines the problem formulation of the nonlinear quarter-car active suspension system and the system requirements. A detailed design method for a time-delayed adaptive neural network controller is shown in Section 3, with the stability analysis being verified. The performance of the TDANNC controller is demonstrated in comparison with the ones of the neural network control (NNC), the TDC, the proportional integral derivative (PID), and the conventional passive system, through simulation results and discussions provided in Section 4. Lastly, Section 5 concludes this work.

2. Nonlinear Quarter-Car Model and System Requirements

2.1 Nonlinear Quarter-Car Active Suspension Model

In this subsection, the nonlinear quarter-car active suspension model, which has been widely

employed in different studies because it is easy to use and can capture many important features of an actual suspension system, is described in detail and shown in Figure 1.

Figure 1 describes the modeling of nonlinear quarter vehicle active suspension, where m_c is the sprung mass (i.e., it represents the chassis of the car), m_w is the unsprung mass (i.e., it displays the weight of the wheel of the car), whereas $F(t)$, $F_s(x_c,x_w,t)$, $F_c(\dot{x}_c,\dot{x}_w,t)$, $F_{kt}(x_w,x_g,t)$, $F_{ct}(\dot{x}_w,\dot{x}_g,t)$ stand for the active control force of the actuator, the spring and damper force of the suspension system and the spring and damper force of the wheel, respectively. The displacements of the body and axle masses are indicated by the symbols x_c and x_w, respectively.

The dynamic model of the sprung and unsprung masses is given as (Pang et al., 2019):

$$\begin{cases} m_c\ddot{x}_c(t) = -F_s(x_c,x_w,t) - F_c(\dot{x}_c,\dot{x}_w,t) + F(t) \\ m_w\ddot{x}_u(t) = F_s(x_c,x_w,t) + F_c(\dot{x}_c,\dot{x}_w,t) - \\ \qquad F_{kt}(x_w,x_g,t) - F_{ct}(\dot{x}_w,\dot{x}_g,t) - F(t) \end{cases} \tag{1}$$

where $\ddot{x}_c(t)$ and $\ddot{x}_w(t)$ are the sprung and unsprung mass accelerations, respectively, and the mathematical expression of $F_s(x_c,x_w,t)$, $F_c(\dot{x}_c,\dot{x}_w,t)$, $F_{kt}(x_w,x_g,t)$, and $F_{ct}(\dot{x}_w,\dot{x}_g,t)$ are defined as follows:

$$F_s(x_c,x_w,t) = k_s(x_c(t)-x_w(t)) + k_{ns}(x_c(t)-x_w(t))^3 \tag{2}$$

$$F_c(\dot{x}_c,\dot{x}_w,t) = \begin{cases} C_{s1}(\dot{x}_c(t)-\dot{x}_w(t)), & (\dot{x}_c(t)-\dot{x}_w(t)) > 0 \\ C_{s2}(\dot{x}_c(t)-\dot{x}_w(t)), & (\dot{x}_c(t)-\dot{x}_w(t)) \le 0 \end{cases} \tag{3}$$

$$F_{kt}(x_w,x_g,t) = k_t(x_w(t)-x_g(t)) \tag{4}$$

$$F_{ct}(\dot{x}_w,\dot{x}_g,t) = C_t(\dot{x}_w(t)-\dot{x}_g(t)) \tag{5}$$

where k_s and k_{ns} are the linear spring rigidity and spatial stiffness coefficients, respectively. k_t represents the tire stiffness coefficient and C_t is the damping coefficient, with C_{s1} and C_{s2} which represent the damping coefficients when extending and compressing the piecewise linear damper, respectively.

The state-space and output equations for quarter vehicle suspension are as follows:

$$\begin{cases} \dot{x}_1(t) = x_2(t) \\ \dot{x}_2(t) = \dfrac{1}{m_c(t)}(-F_s(x_c,x_w,t) - F_c(\dot{x}_c,\dot{x}_w,t) + F(t)) \\ \dot{x}_3(t) = x_4(t) \\ \dot{x}_4(t) = \dfrac{1}{m_w}(F_s(x_c,x_w,t) + F_c(\dot{x}_c,\dot{x}_w,t) - F_{kt}(x_w,x_g,t) \\ \qquad -F_{ct}(\dot{x}_w,\dot{x}_g,t) - F(t)) \end{cases} \tag{6}$$

$m_c(t)$ is always changing due to variations in passenger numbers and vehicle body loads, so it is determined as the uncertain parameters of the control plant in this article, and it is assumed that the lower and upper bounds of $m_c(t)$, denoted as $m_{c\min}$ and $m_{c\max}$, satisfy

$$m_c(t) \in \{m_c(t) : m_{c\min} \le m_c(t) \le m_{c\max} \tag{7}$$

The performance output vector, which contains the relevant system quantities as will be defined later, in subsection 2.2.4, is the following:

$$y(t) = [\ddot{x}_c \quad F_{dyn} \quad x_c - x_w]^T \tag{8}$$

with $F_{dyn} = F_{kt}(x_w,x_g,t) + F_{ct}(\dot{x}_w,\dot{x}_g,t)$, denoting the dynamic wheel load.

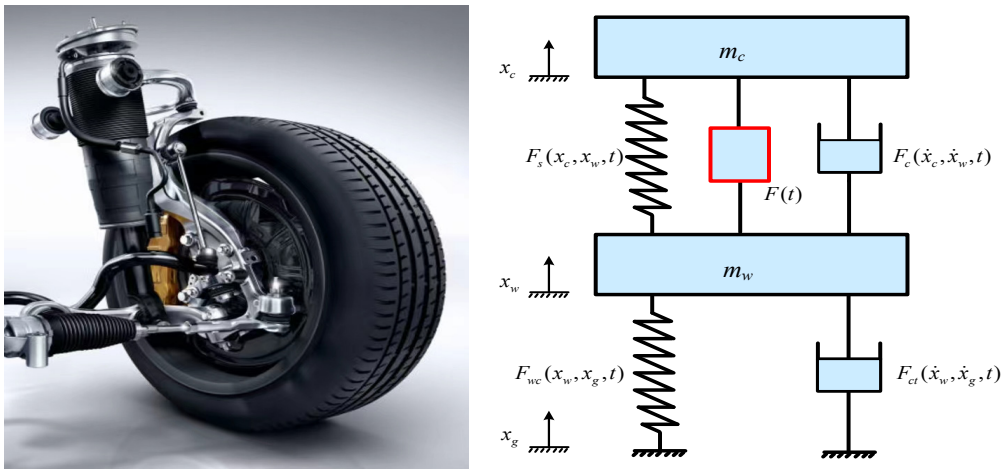

Figure 1. A quarter vehicle active suspension dynamics model

2.2 System Requirements and Performance Evaluation

The following aspects are regarded to be active suspension system performance requirements:

2.2.1 Ride Comfort

As it is well known, the primary function of active suspension control is to design a controller capable of isolating the car body from external disturbances, i.e., minimizing the vertical acceleration of the car to ensure ride comfort.

A simple yet widely used measure for ride comfort is the root mean square (*rms*) value of the vertical body acceleration $\ddot{x}_c(t)_{rms}$ that should be reduced. Similarly, $\max(|\ddot{x}_c(t)|)$ can be evaluated to consider peaks in the chassis acceleration signal, which are especially noticeable during singular disturbance events (Heißing & Ersoy, 2010).

2.2.2 Safety Requirement

For a safe ride, the contact between the tire and the road is essential. As a result, longitudinal and lateral force transfer is made possible, allowing the driver to control the vehicle by applying the brake, steering, and throttle. Therefore, the dynamic wheel load of the *rms* value of a quarter car should be constrained as follows:

$$F_{dyn} < (m_c + m_w)g \tag{9}$$

where g denotes the gravitational constant and $(m_c + m_w)g$ denotes the static wheel load (Mitschke & Wallentowitz, 2004).

2.2.3 Suspension Deflection Requirement

Suspension deflection is well-known to be one of the basic performance requirements for suspension systems, as the large working space of suspension causes damage to vehicle components and increases the passengers' discomfort. Besides, given the importance of suspension deflection on vehicle suspensions, the suspension dynamic displacement should be less than the allowable suspension travel, i.e.,

$$x_{c\text{-}w} = x_c - x_w \le \Delta x_{c\text{-}w\max} \tag{10}$$

where $\Delta x_{c\text{-}w\max}$ represents the maximum value of the suspension deflection. The standard deviation $\|x_c\text{-}x_w\|_{std}$ is utilized for suspension deflection analysis rather than the *rms* value due to the dynamic change in the equilibrium position of the suspension produced by the asymmetric damping characteristic when the suspension is subjected to road-induced vibrations (Koch, Kloiber & Lohmann, 2010).

2.2.4 Performance Evaluation

The achievement of the suspension of all controllers is investigated in order to evaluate the performance of the proposed controller. As a result, the performance gains relative to a reference system are defined as follows:

$$P_{g,obj} = 1 - \frac{\|obj_{cont}\|_i}{\|obj_{ref}\|_i} \tag{11}$$

where $\|obj_{cont}\|_i$ represents the outputs of the controlled active suspension, such as root mean square (rms) value and peak values. Simultaneously, $\|obj_{ref}\|_i$ is the performance of a benchmark suspension that serves as the reference. A positive value of performance gains $P_{g,obj}$ denotes a decrease in the absolute value of the corresponding quantity and thus an improvement in performance (Wang, Mustafa & Tian, 2018).

3. Proposed Time-Delay Adaptive Neural Network Control (TDANNC) Scheme

3.1 Time-Delay Control Structure Design

Time-delay control (TDC) has been determined as a simple, efficient, and effective control strategy for variety of nonlinear plants (Kim et al., 2016). The TDC purposefully employs time-delayed information to eliminate unknown dynamics and unexpected disturbances while inserting the desired dynamics of the plant. The unknown nonlinear function is assumed to not change significantly for a sufficiently brief period of time by the time-delay estimation (TDE) method of the TDC. The TDE technique estimates and removes nonlinearities and uncertainties in the plant by carefully using time-delayed information of control inputs and state derivatives. Consider the second-order time-varying nonlinear dynamical system shown below (Ahmed, Ghous & Mumtaz, 2022):

$$\ddot{z}(t) = \beta(\dot{z}(t), z(t)) + \Gamma(\dot{z}(t), z(t), t, W(t)) + u(t) \tag{12}$$

where $z(t)$ and $u(t)$ denote the state variables and the control vector, whereas $\beta(\dot{z}(t), z(t))$ and $\Gamma(\dot{z}(t), z(t), t, W(t))$ represent the known dynamics and the unknown dynamics, and $W(t)$ represents the disturbance input.

Equation (12) can be rewritten in another expression as follows:

$$\ddot{z}(t) = \Phi(\dot{z}(t), z(t), t) + u(t) \quad (13)$$

with

$$\Phi(\dot{z}(t), z(t), t) = -\beta(\dot{z}(t), z(t)) - \Gamma(\dot{z}(t), z(t), t, W(t)) \quad (14)$$

The main purpose of TDC is to make the output ($y(t) = z(t)$) of the system to follow the desired input trajectory $y^*(t)$. To this end, $e = y^*(t) - y(t)$, $\dot{e} = \dot{y}^*(t) - \dot{y}(t)$, and $\ddot{e} = \ddot{y}^*(t) - \ddot{y}(t)$ were defined firstly. The desired error dynamics is defined as below:

$$\ddot{e}(t) + \Lambda_d \dot{e} + \Lambda_p e = 0 \quad (15)$$

where Λ_d and Λ_p are constant gains, whereas the control input can be selected as:

$$u(t) = u_0 - \hat{\Phi}(\dot{z}(t), z(t), t) \quad (16)$$

with

$$u_0 = \ddot{y}^*(t) + \Lambda_d \dot{e}(t) + \Lambda_p e(t) \quad (17)$$

The TDE, as a core component of TDC, is used to estimate the lumped dynamics $\Phi(\dot{z}(t), z(t), t)$ in a straightforward manner (Mustafa, Wang & Tian, 2019b).

$$\hat{\Phi}(\dot{z}(t), z(t), t) \cong \Phi(\dot{z}(t), z(t), t - \Delta t) \quad (18)$$

where $\Phi(\dot{z}(t), z(t), t - \Delta t)$ is the time-delayed value of $\Phi(\dot{z}(t), z(t), t)$ with delayed time Δt.

From equations (13) – (18), one can get:

$$\hat{\Phi}(\dot{z}(t), z(t), t) = \ddot{z}(t - \Delta t) - u(t - \Delta t) \quad (19)$$

As a result of equations (16) – (19), the TDC law is expressed as follows:

$$u(t) = \ddot{y}^*(t) + \Lambda_d \dot{e}(t) + \Lambda_p e(t) - \ddot{z}(t - \Delta t) + u(t - \Delta t) \quad (20)$$

By substituting equation (20) into equation (13), the error equation can be obtained as follows:

$$\ddot{e}(t) + \Lambda_d \dot{e}(t) + \Lambda_p e(t) + \Phi(\dot{z}(t), z(t), t) - \hat{\Phi}(\dot{z}(t), z(t), t) = 0 \quad (21)$$

Λ_p and Λ_d in the equation mentioned above determine the dynamics of the stable closed-loop error, which can be set using the Hurwitz criterion, while $\Phi(\dot{z}(t), z(t), t) - \hat{\Phi}(\dot{z}(t), z(t), t)$, the estimation error, is mostly bounded. However, because of the time delay Δt, the estimation error does not have to be zero for actual engineering implementation. The estimation error is barely under bound with the required Λ_p and Λ_d. In the following, an adaptive neural network is paired with time-delay control to compensate for the estimation error.

3.2 Proposed TDANNC Scheme

In this part, adaptive neural network control (ANNC) is used as an additional input to counteract the estimation error of the TDE. Figure 2 depicts the related architecture of the suggested technique. The total input signal is expressed as follows:

$$u(t) = \ddot{y}^*(t) + \Lambda_d \dot{e}(t) + \Lambda_p e(t) - \hat{\Phi}(z(t), t) - u_{NN}(t) \quad (22)$$

where $u_{NN}(t)$ is the additional input of the RBF neural network control with an adaptive algorithm. Further, the new closed-loop error can be obtained as below:

$$\ddot{e}(t) + \Lambda_d \dot{e}(t) + \Lambda_p e(t) = \vartheta(z) + u_{NN}(t) \quad (23)$$

where $\vartheta(z)$ denotes the TDE error, which is defined as:

$$\vartheta(z) = \Phi(\dot{z}(t), z(t), t) - \hat{\Phi}(\dot{z}(t), z(t), t) \quad (24)$$

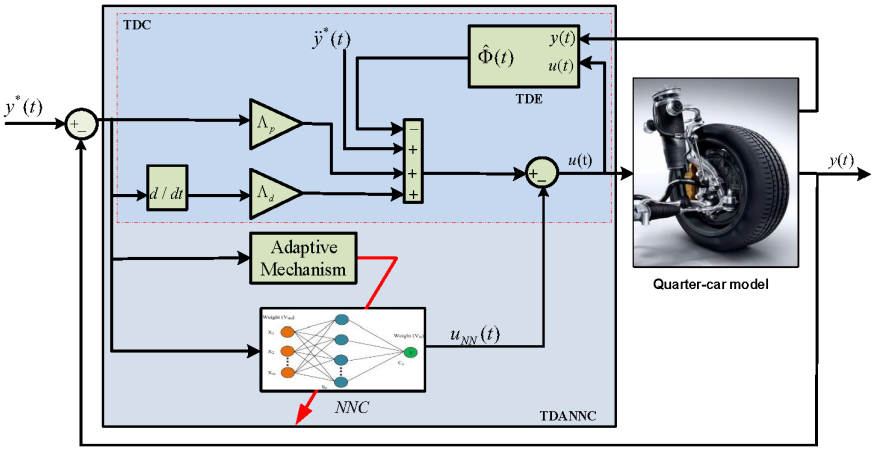

Figure 2. A quarter vehicle active suspension dynamics model

In this paper, an ideal RBF neural network is used to design $\hat{\vartheta}(z)$ in order to approximate $\vartheta(z)$. The algorithm of RBF is represented as follows (Sifaoui et al., 2009):

$$\hat{\vartheta}(z \mid W^*) = W^{*T} h(z) \tag{25}$$

where W^* represents the optimal weight value, that must be met with $W^* = \arg\min\left[sup \left| \hat{\vartheta}(z) - \vartheta(z) \right| \right]$, and $h(z) = \exp\left(-\|z - c\|^2 / 2b^2 \right)$ denotes the Gaussian function for the hidden layer, whereas c and b represent the center and width of the Gaussian function, respectively.

The approximation error can be defined as:

$$\sigma = \vartheta(z) - W^{*T} h(z) \tag{26}$$

where the approximation error σ is mostly bound as $|\sigma| \le \sigma_{\max}$.

The closed-loop error can be obtained by substituting $\vartheta(z)$ from equation (26) into equation (23) as follows:

$$\ddot{e}(t) + \Lambda_d \dot{e}(t) + \Lambda_p e(t) = W^{*T} h(z) + \sigma + u_{NN}(t) \tag{27}$$

To compensate the estimation error, i.e., ($\lim_{t\to\infty} e(t) = 0$), the following equation should be satisfied:

$$u_{NN} = -\hat{\vartheta}(z \mid W^*) = -\hat{W}^T h(z) \tag{28}$$

where $\hat{W}$ denotes the estimated parameter for W. The adaptive law is formulated as follows (Cheng, Hou & Tan, 2009):

$$\dot{\hat{W}} = -\xi E^T P B h(z) \tag{29}$$

where ξ is a positive constant. P and B will be defined later.

The new closed-loop error equation can be expressed as follows:

$$\ddot{e}(t) = -\Lambda_p e(t) - \Lambda_d \dot{e}(t) + W^{*T} h(z) + \sigma + u_{NN}(t) \tag{30}$$

Let

$$\begin{cases} \psi = \begin{bmatrix} 0 & 1 \\ -\Lambda_p & -\Lambda_d \end{bmatrix} \\ B = \begin{bmatrix} 0 \\ 1 \end{bmatrix} \end{cases} \tag{31}$$

Now, equation (30) can be rewritten as follows:

$$\dot{E} = \psi E + B[W^* - \hat{W})^T h(z) + \sigma] \tag{32}$$

Design a Lyapunov function such as:

$$V = \frac{1}{2} E^T P E + \frac{1}{2\xi} (W^* - \hat{W})^T (W^* - W) \tag{33}$$

where $W^* - \hat{W}$ represents the parameter estimation error, and P is the positive-definite symmetric matrix, which satisfies the following Lyapunov equation.

$$\psi^T P + P\psi = -\Gamma \tag{34}$$

with $\Gamma \ge 0$, and ψ is given by equation (31).

Now, let $\kappa = B[W^* - \hat{W})^T h(z) + \sigma]$, equation (32) can be rewritten as follows:

$$\dot{E} = \psi E + \kappa \tag{35}$$

Then,

$$\dot{V} = \frac{1}{2} \dot{E}^T P E + \frac{1}{2} E^T P \dot{E} + \frac{1}{\xi} (W^* - \hat{W})^T \dot{W} \tag{36}$$

By substituting $\dot{E}$ from equation (35) into equation (36), one can obtain

$$\begin{aligned} \dot{V} &= \frac{1}{2} \left(E^T \psi^T + \kappa^T \right) P E + \frac{1}{2} E^T P \left(\psi E + \kappa \right) \\ &\quad + \frac{1}{\xi} (W^* - \hat{W})^T \dot{W} \\ &= \frac{1}{2} E^T \left(\psi^T P + P\psi \right) E + \frac{1}{2} \kappa^T P E \\ &\quad + \frac{1}{2} E^T P \kappa + \frac{1}{\xi} (W^* - \hat{W})^T \dot{W} \end{aligned} \tag{37}$$

Now, by substituting equation (34) into equation (37), one obtains:

$$\begin{aligned} \dot{V} &= -\frac{1}{2} E^T \Gamma E + \frac{1}{2} \left(\kappa^T P E + E^T P \kappa \right) \\ &\quad + \frac{1}{\xi} (W^* - \hat{W})^T \dot{W} \\ &= -\frac{1}{2} E^T \Gamma E + E^T P \kappa \\ &\quad + \frac{1}{\xi} (W^* - \hat{W})^T \dot{W} \end{aligned} \tag{38}$$

By adding κ into the above equation, noting that $E^T P B (\hat{W} - W^*)^T h(z) = (W - W^*)^T \left[E^T P B h(z) \right]$, one can obtain:

$$\begin{aligned} \dot{V} &= -\frac{1}{2} E^T \Gamma E + E^T P B (W^* - \hat{W})^T h(z) \\ &\quad + E^T P B \sigma + \frac{1}{\xi} (W^* - \hat{W})^T \dot{W} \\ &= -\frac{1}{2} E^T \Gamma E + E^T P B \sigma \\ &\quad + \frac{1}{\xi} (W^* - \hat{W})^T \left[\dot{W} + \xi E^T P B h(z) \right] \end{aligned} \tag{39}$$

By substituting the adaptive law equation (29) into the above, one can obtain:

$$\dot{V} = -\frac{1}{2} E^T \Gamma E + E^T P B \sigma \tag{40}$$

Since $-\frac{1}{2}E^T\Gamma E \le 0$, therefore, the approximate error σ^2 can be sufficiently reduced by the adaptive neural network compensator, in order to obtain $\dot{V} \le 0$.

Then it can be observed that E and $W^* - \hat{W}$ are all limited. The convergence is formulated as follow:

$$\|E\| \le \frac{2\lambda_{\max}(PB)\sigma_{\max}}{\lambda_{\min}(\Gamma)} \tag{41}$$

where $\lambda(\cdot)$ is the characteristic value, whereas $\lambda_{\max}$ and $\lambda_{\min}$ are the maximum and minimum value of matrix, respectively.

4. Simulation Results and Discussion

The main purpose of car active suspension control is to reduce the acceleration of the body of the car in order to enhance the ride comfort. while keeping acceptable limits for both suspension deflection and dynamic wheel load, in order to guarantee ride safety. In this section, the TDANNC strategy is tested based on the quarter-car active suspension model depicted in Figure 1. Numerical results are provided to demonstrate the efficiency of the control method described in this paper by comparing the performances of the conventional passive system, of the PID, of the TDC, and of the NNC controllers with that of the proposed controller.

The quarter-car model is widely acknowledged as adequate for examining some suspension performance targets (Tusset, Rafikov & Balthazar, 2009). The quarter-car model illustrated in Figure 1 has the model parameters listed in Table 1. Two degrees of freedom (2DF) for vertical motion of the sprung and unsprung masses are taken into consideration in this work.

The parameters of TDANNC controller were set as follows:

$\Lambda_p = 10.1409$, $\Lambda_d = 8.1413$, $\xi = 1200$, $\Gamma = \begin{bmatrix} 0 & 1000 \\ 1000 & 0 \end{bmatrix}$ and $t_d = 0.001\text{sec}$. The initial weight value is set to zero, while the c_{ij} and b_j parameters of the Gaussian function are specified as $\begin{bmatrix} -2 & -1 & 0 & 1 & 2 \end{bmatrix}$ and 1.0, respectively. The TDC and NNC parameters have the same values as the TDANNC parameters. In contrast, PID parameters are $k_p = 5.4068$, $k_i = 3.2513$, and $k_d = 0.0056$.

Note: All of the parameters used in this work were calculated using particle swarm optimization (PSO); for more information on PSO, see the work of Mustafa, Wang & Tian (2019b) and the references therein.

The simulation experiments are carried out for three distinct road profiles, namely:

Case 1: To demonstrate the efficacy of the proposed control law, the typical bump road is considered as the road disturbance. The typical bump road input is described in (Mitschke & Wallentowitz, 1972) as follows:

$$x_g = \begin{cases} h(1-\cos(\frac{2\pi v_b}{L}\text{t})), & \text{for } 0, \le \text{t} \le \frac{L}{v_b} \\ 0, & else \end{cases} \tag{42}$$

where h is half of the bump height $\hat{h}$, L is the bump length and v_b is the speed of the vehicle passing by.

Case 2: The resonance frequency of the body of the car is approximately 4 Hz, so an external excitation at or near this frequency could result in an undesirable oscillation. The sinusoidal road profile (see (Mustafa, Wang, & Tian, 2019b)) is

Table 1. The quarter-car model parameters

Model parameter	Symbol	Value	Unit
Sprung mass	m_c	94.38	kg
Unsprung mass	m_w	23.92	kg
Primary spring stiffness	c_c	8400	N/m
Linear tire stiffness	c_w	152186	N/m
Friction force spring/damper	$F_{f,1}$	115	N
Friction scaling spring/damper	$k_{f,1}$	125	sec/m
Friction force chassis mass guides	$F_{f,2}$	20	N
Friction scaling chassis mass guides	$k_{f,2}$	125	sec/m
Tire damping coefficient	d_w	50	Nsec/m

used to evaluate the effectiveness of the controller at frequencies close to the natural resonance of the system. The sinusoidal road input is represented as follows:

$$x_g = 0.006 \sin 2\pi t \tag{43}$$

***Case 3**:* The random profile is selected in order to show the effectiveness of the proposed control law. In this case, a class D road profile is chosen; the random road input is represented by equation (44) as (Mustafa, Wang, & Tian, 2019a):

$$\dot{x}_g(t) = -2\pi f_0 v x_g(t) + 2\pi n_0 \sqrt{G_q(n_0)} v w(t) \tag{44}$$

where f_0 denotes the cutoff frequency of the road space, v is speed of the vehicle, n_0 is the spatial reference frequency, $G_q(n_0)$ is the power spectral density of the road profile, and $w(t)$ is the input white noise. The random road excitation is shown in Figure 3.

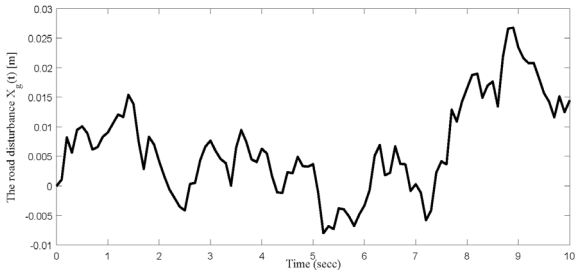

Figure 3. The random road profile

4.1 Results and Discussion of the Bump Road Surface

Using TDANNC, NNC, TDC, PID controllers, and the conventional passive system, the dynamic response of the sprung mass acceleration, the tire deflection, and the dynamic wheel load during a car crossing over the bump road excitation are illustrated in Figures 4–6.

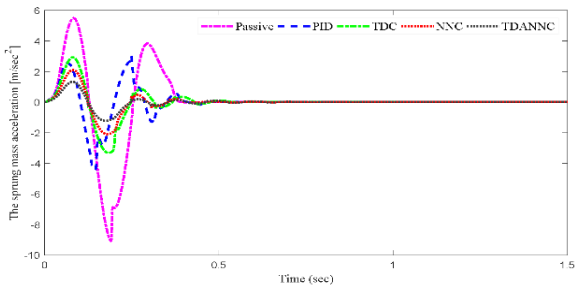

Figure 4. Sprung mass acceleration response under bump road excitation

The sprung mass acceleration response for various control strategies is shown in Figure 4. The highest values for the suggested controller, NNC, TDC, PID, and the conventional passive system, given in meters per square second, are 1.3275, 2.1086, 2.9339, 3.0265, and 5.4958, respectively. With the suggested controller, the body acceleration has a numerical *rms* value of 0.3431 m, compared to 0.5611 m of NNC, 0.8267 m of TDC, 0.8928 m of PID, and 2.0695 m of the conventional passive system. Additionally, as compared to NNC, TDC, PID, and the passive system, the *rms* value of the body acceleration is reduced by the TDANNC by 38.85 %, 58.5 %, and 61.67 %, and by 83.42 %, respectively. When compared to existing controllers, it can be observed that the suggested controller exhibits a considerably quicker decline in the amplitude of the vehicle body acceleration, which would result in much improved ride comfort.

As shown in Figure 5, the proposed controller reduces the peak-to-peak value of the suspension deflection. The maximum suspension deflection value of TDANNC is 0.0103 m.

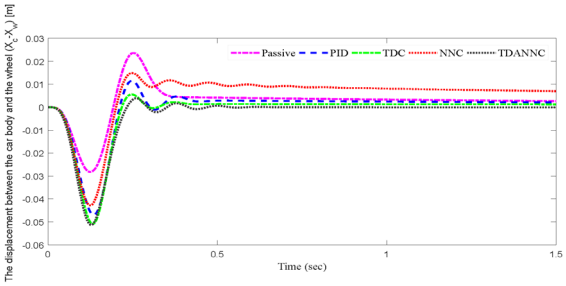

Figure 5. Suspension deflection under bump road excitation

In contrast, it is 0.0149 m, 0.0115 m, 0.0185 m, and 0.0236 m for NNC, PID, TDC, and the conventional passive system, respectively. Meanwhile, the suspension deflection of the TDANNC is smaller than that of the other controllers. Furthermore, the steady-state error is reduced to zero, resulting in much improved vertical motion. Meanwhile, the supplied control action keeps the suspension deflection below the acceptable limit.

The dynamic wheel load response under bump road excitation is shown in Figure 6. The TDANNC controller performs a perfect result, by enabling both the steady-state error to rapidly tend to zero with a tolerable overshoot, and the driver to steer, brake, and accelerate the vehicle. For the TDANNC, NNC, TDC, PID, and passive systems, the maximum values of the dynamic

wheel load signals expressed in Newtons are 588.6025, 627.0944, 674.7201, 707.5472 and 789.0074, respectively.

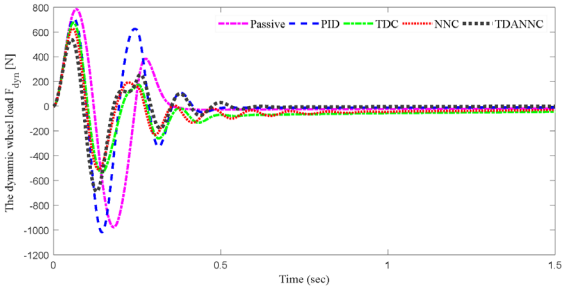

Figure 6. Dynamic wheel load response under bump road excitation

4.2 Results and Discussion of the Sinusoidal Road Surface

The dynamic responses of sprung mass acceleration using the passive system, PID, TDC, NNC, and TDANNC controllers are shown in Figure 7 when the vehicle passes over the sinusoidal road excitation. It can be observed that the amplitude of the vertical acceleration of the body of the car decreases much more rapidly in the proposed controller compared to other controllers; this will result in a significantly more comfortable ride.

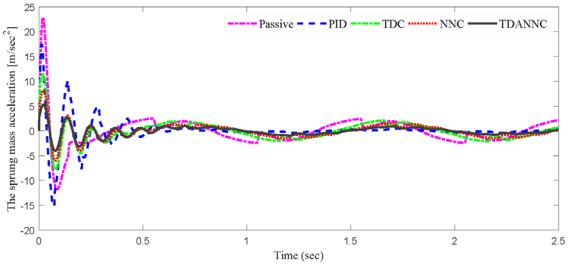

Figure 7. Sprung mass acceleration response under sinusoidal road excitation

4.3 Results and Discussion about the Random Road Surface

Figure 8 shows the dynamic response values of the sprung mass acceleration in the case of random road stimulation. From this figure, it can be observed that the suggested method has the lowest amplitude levels compared to other methods. The TDANNC minimizes the maximum *rms* values of the sprung mass acceleration by 26.14%, 7.58%, 49.24%, and 56.51% relative to NNC, TDC, PID, and the passive system, respectively. For the tire deflection and dynamic wheel load responses, all controllers demonstrate an appropriate restriction that satisfies ride safety requirements. The results demonstrate again that an active vehicle suspension system controlled by TDANNC can provide a good reaction that fulfills the stability of the automobile and a better response in terms of ride comfort.

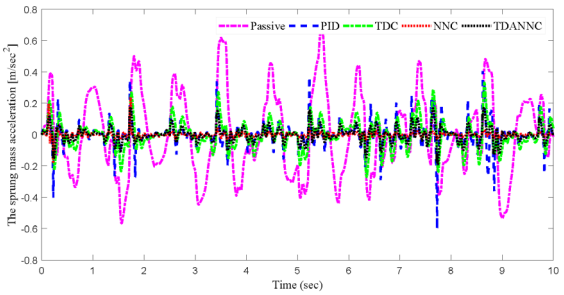

Figure 8. Sprung mass acceleration response under random road excitation

Besides, according to International Organization for Standardization (ISO) 2361, the sprung mass acceleration of a vehicle system in the frequency range between 4-10 Hz must be minimized to improve ride comfort (Li, Jing & Karimi, 2014). Due to this factor, the results obtained for sinusoidal and random road excitations are presented in the frequency domain. Figures 9 and 10 depict the modulus of the Fast Fourier Transform (FFT) of the sprung mass acceleration response from 0 to 10 Hz for sinusoidal and random road excitations, respectively.

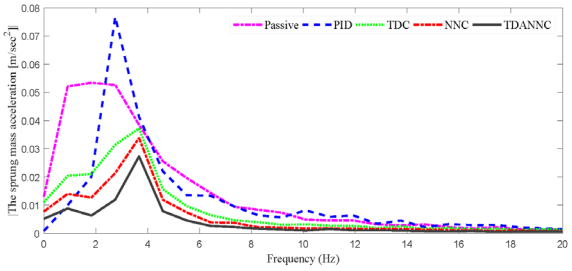

Figure 9. Sprung mass acceleration (amplitude vs. frequency) under sinusoidal road excitation

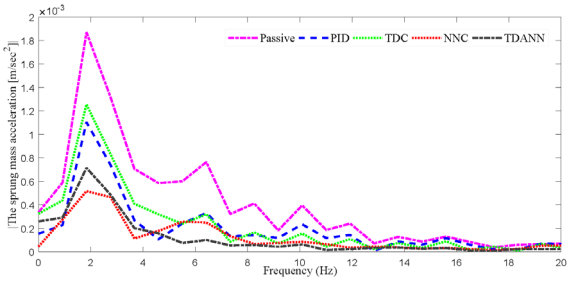

Figure 10. Sprung mass acceleration (amplitude vs. frequency) under random road excitation

4.4 Measurement Results and Discussion

To assess the proposed controller, the suspension performances of all controllers are visualized in spider charts. The resultant performance advantages with regard to the passive suspension system are displayed in the spider charts in Figures 11–13, for bump, sinusoidal, and random road profiles, respectively, based on the performance gains indicated in subsection 2.2.4 and equation (11).

It should be noted that the essential performance criteria for ride comfort and vehicle stability are car body acceleration $\ddot{x}_c(t)$, suspension deflection $x_c(t)-x_w(t)$, and dynamic wheel load $F_{dyn}(t)$. Therefore, the primary objectives are to reduce $\ddot{x}_c(t)$, x_c-x_w, and $F_{dyn}(t)$ in order to enhance vehicle stability and ride quality.

Figure 11 displays the results according to the bump road profile; numerically, the proposed technique may greatly enhance ride comfort and safety. It is evident that the TDAFLC technique performs better than other controllers when compared to them in terms of $\max(\ddot{x}_c)$, $\|\ddot{x}_c\|_{rms}$, $\min(\ddot{x}_c)$, $\max(x_c-x_w)$ and $\|x_c-x_w\|_{std}$. On the other hand, the suggested approach produces excellent responses in terms of $\max(F_{dyn})$ and $\|F_{dyn}\|_{rms}$, guaranteeing that the suspension performances do not go beyond the boundary limits stated in subsection 2.2.

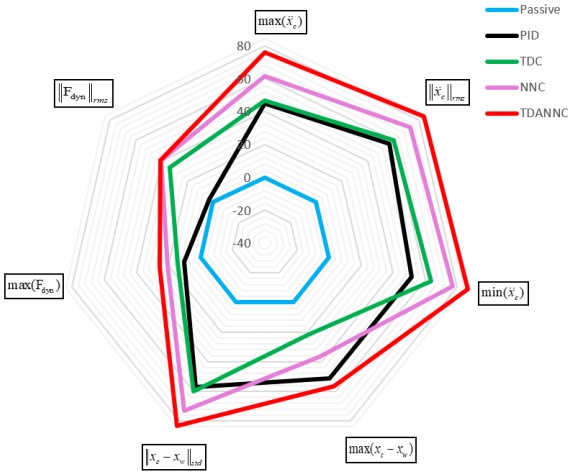

Figure 11. The controller performance measurement results under bump road profile

The controller performance measurement results for the active suspension system under the sinusoidal road profile are shown in Figure 12. It becomes clear that the proposed controller meets all the performance criteria with excellent results. Performance measurements of all the controllers on the random road profile are shown in Figure 13. Again, it is obvious that the proposed controller achieves superb results across the board in terms of performance requirements. It should be noted that performance degradations in suspension deflection ($\max(x_c-x_w)$ in Figure 12 and $\|x_c-x_w\|_{std}$ in Figure 13) are unimportant for all controllers because the passive reference exhibits extremely low suspension deflections.

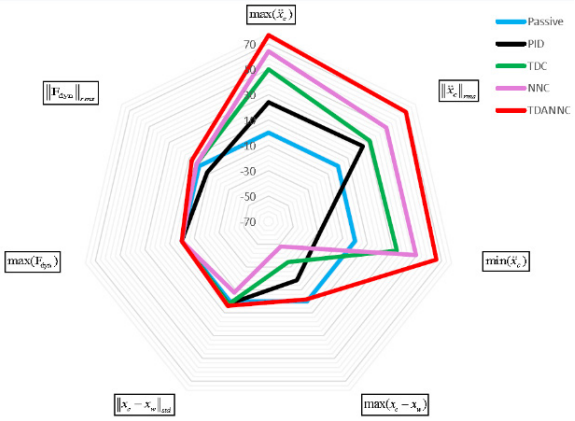

Figure 12. The controller performance measurement results under sinusoidal road profile

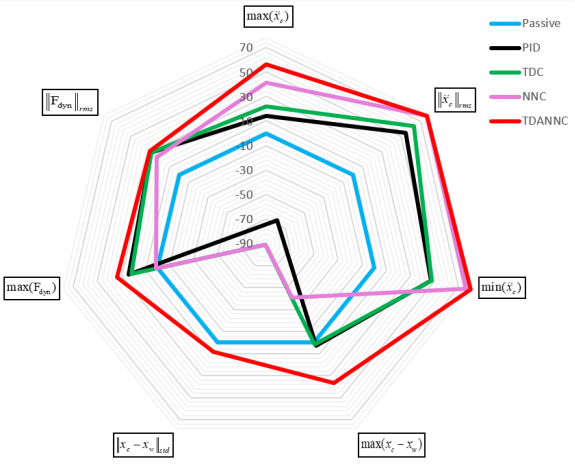

Figure 13. The controller performance measurement results under random road profile

Even with varying road inputs, from Figures 11 – 13, it becomes evident that the TDANNC method substantially improves the ride comfort and safety. Based on the results of the measurements, it is clear that the TDANNC method effectively provides sufficient suspension deflection space and minimal car-body acceleration while maintaining good dynamic wheel load responses. The suggested controller ensures safety and comfort for all three road profiles.

When the amplitude of the bumpy road surface is raised by 25 %, the performance advantage of TDANNC is further boosted. While retaining the rms limitations for dynamic wheel load and suspension deflection, the suggested controller may improve ride comfort by 30.25 %. However, other controllers violate the restrictions for dynamic wheel load and/or suspension deflection.

5. Conclusion

This paper proposes a new time-delay adaptive neural network control (TDANNC) to resolve the classic conflict between improving car ride comfort and keeping ride safety within an acceptable safety limit. The TDANNC comprises three parts: First, the model nonlinearity and external disturbances are replaced based on time-delay control. Second, a radial basis function neural network is added to time-delay control to obtain a compelling tracking trajectory. Third, an adaptive law mechanism is used to achieve excellent overall performance across various road profiles, which can quickly and precisely adjust the neural network control gain online based on the control error. Under three different types of road disturbances, the performance of the proposed TDANNC is evaluated and contrasted with that of the conventional passive system, TDC, PID, and NNC controllers. The simulation results demonstrate the effectiveness and success of the proposed strategy. It can be concluded that the proposed controller improves ride comfort while ensuring ride safety, thus enhancing the performance of the active suspension system.

Acknowledgements

The research reported in this paper has been supported by Natural Science Foundation of Shandong Province under Grant ZR2021ME236, and by the Science and Technology Innovation Key Research and Development Project of Yantai City under Grant 2021XDHZ070.

REFERENCES

Ahmed, S., Ghous, I. & Mumtaz, F. (2022). TDE Based Model-free Control for Rigid Robotic Manipulators under Nonlinear Friction, *Scientia Iranica, 25*, 2628-2642. DOI: 10.24200/SCI.2022.57252.5141

Cao, J., Li, P. & Liu, H. (2010). An interval fuzzy controller for vehicle active suspension systems, *IEEE Transactions on Intelligent Transportation Systems*, *11*(4), 885-895.

Cheng, L., Hou, Z.-G. & Tan, M. (2009). Adaptive neural network tracking control for manipulators with uncertain kinematics, dynamics and actuator model, *Automatica*, *45*(10), 2312-2318.

Dragomir, O., Dragomir, F., Stefan, V. & Minca, E. (2015). Adaptive Neuro – Fuzzy Inference Systems– An Alternative Forecasting Tool for Prosumers. *Studies in Informatics and Control*, *24*(3), 351-360. DOI: 10.24846/v24i3y201511

Fleps-Dezasse, M., Bünte, T., Svaricek, F. & Brembeck, J. (2018). LPV feedforward control of semi-active suspensions for improved roll stability, *Control Engineering Practice*, *78*, 1-11.

Gokul Prassad, S. & Malar Mohan, K. (2019). A contemporary adaptive air suspension using LQR control for passenger vehicles*, ISA Transactions*, *93*, 244-254.

He, H., Li, Y., Jiang, J. Z., Burrow, S., Neild, S. & Conn, A. (2021). Using an inerter to enhance an active-passive-combined vehicle suspension system, *International Journal of Mechanical Sciences*, *204*, article ID: 106535.

Heißing, B. & Ersoy, M. (Eds.). (2010). *Chassis Handbook: Fundamentals, Driving Dynamics, Components, Mechatronics, Perspectives.* Springer Science & Business Media.

Hu, J.-W. & Lin, J.-S. (2008). Nonlinear control of full-vehicle active suspensions with backstepping design scheme, *IFAC Proceedings Volumes*, *41*(2), 3404-3409.

Jin, M., Kang, S. H., Chang, P. H. & Lee, J. (2017). Robust control of robot manipulators using inclusive and enhanced time delay control, *IEEE/ASME Transactions on Mechatronics*, *22*(5), 2141-2152.

Kim, J., Joe, H., Yu, S.-C., Lee, J. S. & Kim, M. (2016). Time-delay controller design for position control of autonomous underwater vehicle under disturbances, *IEEE Transactions on Industrial Electronics*, *63*(2), 1052-1061.

Koch, G., Kloiber, T. & Lohmann, B. (2010). Nonlinear and filter-based estimation for vehicle suspension control. In *2010 49th IEEE Conference on Decision and Control (CDC)*, (pp. 5592-5597).

Li, H., Jing, X. & Karimi, H. R. (2014). Output-Feedback-Based H∞ Control for Vehicle Suspension Systems with Control Delay, *IEEE Transactions on Industrial Electronics*, *61*(1), 436-446.

Long, G., Ding, F., Zhang, N., Zhang, J. & Qin, A. (2020). Regenerative active suspension system with residual energy for in-wheel motor driven electric vehicle, *Applied Energy*, *260*, article ID: 114180.

Mefoued, S. (2015). A second order sliding mode control and a neural network to drive a knee joint actuated orthosis, *Neurocomputing*, *155*, 71-79.

Mitschke, M. & Wallentowitz, H. (1972). *Dynamik der Kraftfahrzeuge*, *vol. 4*, 183-187. Springer.

Mitschke, M. & Wallentowitz, H. (2004). *Einführung Dynamik der Kraftfahrzeuge*, 1-4. Springer.

Mustafa, Ghazally I. Y., Wang, H. & Tian, Y. (2019a). Model-free Adaptive Fuzzy Logic Control for a Half-car Active Suspension System, *Studies in Informatics and Control, 28*(1), 13-24. DOI: 10.24846/v28i1y201902.

Mustafa, Ghazally I. Y., Wang, H. & Tian, Y. (2019b). Vibration control of an active vehicle suspension systems using optimized model-free fuzzy logic controller based on time delay estimation, *Advances in Engineering Software, 127*, 141-149.

Mustafa, Ghazally I. Y., Wang, H. & Tian, Y. (2020). Optimized fast terminal sliding mode control for a half-car active suspension system, *International Journal of Automotive Technology, 21*(4), 805-812.

Pan, H., Sun, W., Jing, X., Gao, H. & Yao, J. (2017). Adaptive tracking control for active suspension systems with non-ideal actuators, *Journal of Sound and Vibration*, *399*, 2-20.

Pang, H., Zhang, X., Chen, J. & Liu, K. (2019). Design of a coordinated adaptive backstepping tracking control for nonlinear uncertain active suspension system, *Applied Mathematical Modelling*, *76*, 479-494.

Shehata, A., Metered, H. & Oraby, W. A. (2015). Vibration control of active vehicle suspension system using fuzzy logic controller. In Sinha, Jyoti K. (Ed.), *Vibration Engineering and Technology of Machinery, Mechanisms and Machine Science, vol 23*, 389-399. Springer.

Sifaoui, A., Abdelkrim, A., Alouane, S. & Benrejeb, M. (2009). On new RBF neural network construction algorithm for classification, *Studies in Informatics and Control*, *18*(2), 103-110.

Sun, W., Pan, H., Zhang, Y. & Gao, H. (2014). Multi-objective control for uncertain nonlinear active suspension systems, *Mechatronics*, *24*(4), 318-327.

Tusset, A. M., Rafikov, M. & Balthazar, J. M. (2009). An intelligent controller design for magnetorheological damper based on a quarter-car model, *Journal of Vibration and Control*, *15*(12), 1907-1920.

Wang, H. P., Mustafa, Ghazally. I. Y. & Tian, Y. (2018). Model-free fractional-order sliding mode control for an active vehicle suspension system, *Advances in Engineering Software*, *115*, 452-461.

Wang, R., Jing, H., Karimi, H. R. & Chen, N. (2015). Robust fault-tolerant H∞ control of active suspension systems with finite-frequency constraint, *Mechanical Systems and Signal Processing*, *62*, 341-355.

Xia, W., Zhu, J.-l., Jiang, W.-Y. & Zhu, L.-F. (2016). An enhanced mixed modulated Lagrange explicit time delay estimator with noisy input, *Frontiers of Information Technology & Electronic Engineering*, *17*, 1067-1073.

Zhao, F., Ge, S. S., Tu, F., Qin, Y. & Dong, M. (2016). Adaptive neural network control for active suspension system with actuator saturation, *IET control theory & applications*, *10*(14), 1696-1705.